Characterization of Calcium, Nucleotide, Phosphate, and Vanadate Bound States by Derivatization of Sarcoplasmic Reticulum ATPase with ThioGlo1

Suming Hua,* Daniele Fabris,[#] and Giuseppe Inesi*
*Department of Biochemistry and Molecular Biology, University of Maryland School of Medicine Baltimore, Maryland 21201, and
[#]Department of Chemistry, University of Maryland Baltimore County, Catonsville, Maryland 21228 USA

ABSTRACT   Sarcoplasmic reticulum vesicles were incubated with the maleimide-directed probe ThioGlo1, resulting in ATPase inactivation. Reacted ThioGlo1, revealed by its enhanced fluorescence, was found to be associated with the cytosolic but not with the membrane-bound region of the ATPase. The dependence of inactivation on ThioGlo1 concentration suggests derivatization of approximately four residues per ATPase, of which Cys^{364}, Cys^{498}, and Cys^{636} were identified in prominently fluorescent peptide fragments. These cysteines reside within the phosphorylation and nucleotide-binding region of the ATPase. Accordingly, protection is observed in the presence of ATP, 2′(3′)-O-(2,4,6-trinitrophenyl)adenosine 5′-diphosphate (TNP-AMP), or an fluoroisothiocyanate label of Lys^{515}. Furthermore, protection is observed in the presence of vanadate (or decavanadate), but not in the presence of phosphate. Labeling occurs equally well in the presence or in the absence of Ca^{2+} and thapsigargin, excluding a role of the E1-to-E2 transition in the protective effect of vanadate. It is concluded that protection by vanadate is due to formation of a pentacoordinated orthovanadate complex at the phosphorylation site, corresponding to a stable transition state analog of the phosphorylation reaction, with intermediate characteristics of the EP1 and EP2 states. The lack of protection by phosphate is attributed to instability of its complex with the enzyme (EP2). These findings are discussed with respect to different structural images obtained from diffraction studies of ATPase in the presence or in the absence of Ca^{2+} and/or decavanadate (Ogawa et al., 1998, *Biophys. J.* 75:41–52).

INTRODUCTION

Functional studies have shown that a fundamental feature of the sarcoplasmic reticulum (SR) Ca^{2+} transport ATPase is the interconversion of two discrete enzyme states (deMeis and Vianna, 1979). The E1 state is induced by Ca^{2+} binding to high-affinity sites exposed to the cytosolic side of the SR membrane, whereas the E2 state is prevalent in the absence of Ca^{2+}. In the presence of Ca^{2+}, E1 is converted to a low Ca^{2+} affinity state after enzyme phosphorylation with ATP, whereby the bound Ca^{2+} is released from the lumenal side of the SR membrane. This interconversion of functional states must be based on a corresponding structural transition, because a long-range intramolecular linkage between a phosphorylation site in the cytosolic region and a Ca^{2+}-binding site in the transmembrane region of the enzyme is required for functional coupling (Inesi et al., 1992b). In recent diffraction studies, large differences were noted in the cytosolic region of ATPase images, depending on whether the images were derived from crystals obtained in the presence of Ca^{2+} or from crystals obtained in the absence of Ca^{2+} and in the presence of vanadate (Ogawa et al., 1998). If these two crystalline states were to correspond to the E1 and E2 states, respectively, the observed differ-

ences would provide a structural counterpart for the well-defined functional characteristics of E1 and E2.

Several studies (Murphy, 1976, 1978; Green et al., 1977; Saito-Nakatsuka et al., 1987; Yamasaki et al., 1990; Squier et al., 1987; Bigelow and Inesi, 1991) have demonstrated changes in the reactivity of various sulfhydryl groups of the SR ATPase, depending on the absence or the presence of various ligands, and on the type of derivatization reagents. We describe here the effects of pertinent ligands on the derivatization of the ATPase cytosolic region with the new maleimide-directed label ThioGlo1. We find that ATP, 2′(3′)-O-(2,4,6-trinitrophenyl)adenosine 5′-diphosphate (TNP-AMP), fluoroisothiocyanate (FITC), and vanadate protect ATPase from derivatization with ThioGlo1. However, derivatization occurs equally well in the presence or in the absence of Ca^{2+}, phosphate, and/or thapsigargin. These effects are helpful in defining various conformational states of the enzyme, independent of crystallization requirements.

MATERIALS AND METHODS

SR vesicles were prepared from rabbit leg skeletal muscle as described by Eletr and Inesi (1972). Protein concentration was determined by the method of Lowry (Lowry et al., 1951). In all cases, to block fast reacting sulfhydryl groups (Murphy, 1978; Saito-Nakatsuka et al., 1987), the SR vesicles were incubated (10 mg SR protein/ml) with 0.05 mM *N*-ethylmaleimide in 20 mM 3-(*N*-morpholino)propanesulfonic acid (MOPS) (pH 7.0), 80 mM KCl, 5 mM $MgCl_2$, for 30 min in ice. The reaction mixture was then diluted to 3.0 mg SR protein/ml, using the medium required for the subsequent derivatization reaction.

Derivatization of the ATPase with FITC was obtained by incubating 3.0 mg SR protein/ml in a medium identical to that used for preincubation with NEM, but containing 4 mM FITC. After 2 min at 25°C, the vesicles were
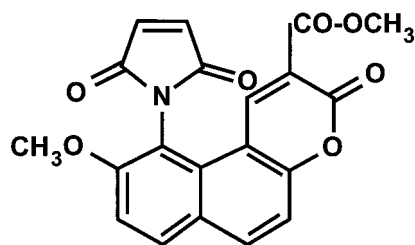
FIGURE 1 Structure of ThioGlo1: ^{3}H-Naphtol[2,1-b]pyran-2-carboxylic acid, 10-(2,5-dihydro-2,5-dioxo-[1]H-pyrrol-1-yl)-9-methoxy-3-oxo-, methyl ester.

centrifuged at $110,000 \times g$ for 45 min, and the sediment was suspended in the usual medium at a concentration of 3.0 mg/ml.

ThioGlo1 (Fig. 1) was purchased from Covalent Associates (Woburn, MA). Derivatization of SR ATPase was obtained by incubating SR vesicles with various concentrations of ThioGlo1 at 25°C in reaction media as described in the figures. The stoichiometry of derivatization was estimated by taking advantage of the fluorescent signal developed by ThioGlo1 after reaction with sulfhydryl moieties and determining the ThioGlo1 missing from the incubation medium. For this purpose, control and derivatized vesicles were separated from the medium by centrifugation ($110,000 \times g$ for 60 min), and the residual ThioGlo1 in the supernatant was incubated with 0.3 mM glutathione for 15 min at 25°C. The resulting fluorescence was measured with 379-nm excitation, at 490-nm emission wavelength. A standard curve was obtained with a known amount of glutathione in the presence of excess ThioGlo1. Alternatively, the fluorescence of the label was determined directly on the SR vesicles or tryptic fragments, using a Jasco spectrofluorometer (FP-777).

Aqueous solutions of ammonium metavanadate (10 mM) were made at pH 2.0, 7.0, or 10.0, adjusted with HCl or NaOH. The solution at pH 2.0 contains mostly decavanadate, whereas the solution at pH 10.0 contains mostly orthovanadate (Fig. 2). ATPase activity was measured under the conditions described in Fig. 3. The inorganic phosphate produced by ATP hydrolysis was determined by the method of Lanzetta et al. (1979).

SDS gel electrophoresis was carried out according to the method of Weber and Osborn (1969). Protein staining was obtained with Coomassie
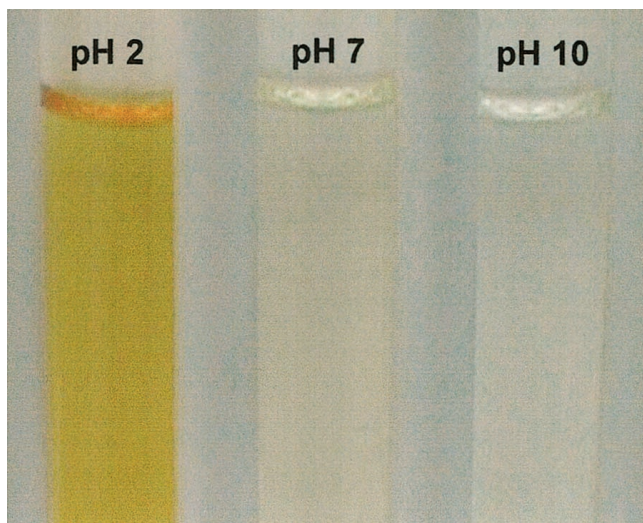

FIGURE 2 Solutions of vanadate at various pH levels. Aqueous solutions were made to 1 mM concentration with metavanadate, and the pH was adjusted with HCl or NaOH. The color of the acid solution is due to the presence of decavanadate.
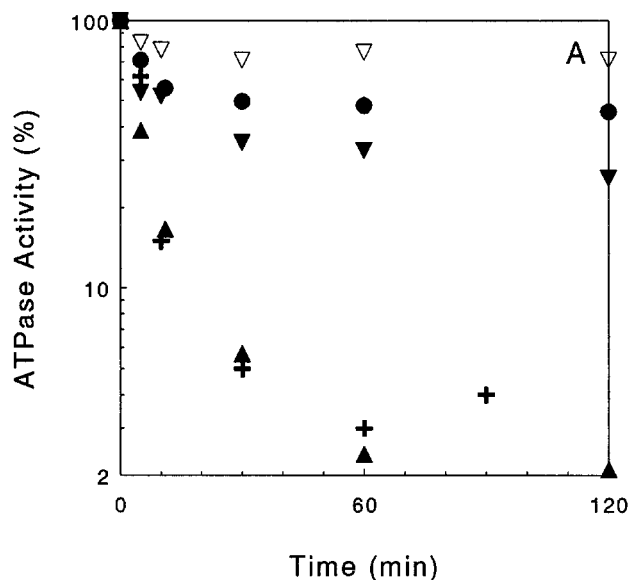

FIGURE 3 Inactivation of SR ATPase by ThioGlo1. The SR vesicles (10.0 mg/ml) were pretreated with 50 μM NEM for 30 min in ice, in the presence of 20 mM MOPS (pH 7.0), 80 mM KCl, and 5 mM MgCl$_2$. The pretreated vesicles were then diluted to yield a reaction mixture containing 20 mM MOPS (pH 7.0), 80 mM KCl, 5 mM MgCl$_2$, 1.0 mM EGTA, 3.0 mg SR protein/ml, and various concentrations of ThioGlo1 ($\triangledown$, 27 μM; $\bullet$, 58 μM; $\blacktriangledown$, 76 μM; $+$, 100 μM; $\blacktriangle$, 212 μM), at 25°C temperature. At the indicated times, samples were collected for determination of ThioGlo1 derivatization stoichiometry (see Materials and Methods) and measurements of ATPase activity. The ATPase reaction mixture contained 5 μg SR protein/ml, 20 mM MOPS (pH 6.8), 80 mM KCl, 3.0 mM MgCl$_2$, 0.2 mM CaCl$_2$, 0.2 mM EGTA, 5 mM sodium azide, 3.0 μM A23187 calcium ionophore, and 3.0 mM ATP, at 37°C temperature. (A) Time dependence of ATPase inactivation at various ThioGlo1 concentrations. (B) Residual ATPase activity as a function of ThioGlo1 derivatization stoichiometry.

blue. The fluorescence of the protein bands was detected and recorded with a NucleoVision imaging apparatus.

Peptide fragments for mass spectrometry were obtained by extensive trypsin digestion of ThioGlo1-labeled SR vesicles and incubation of 4.0 mg
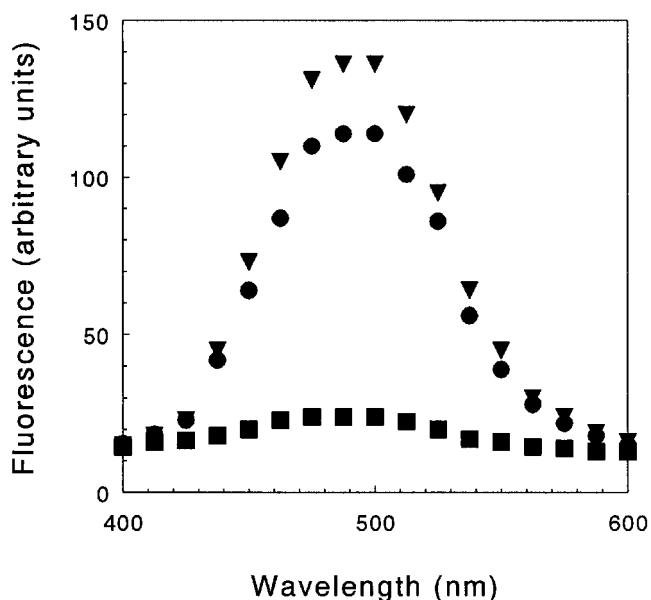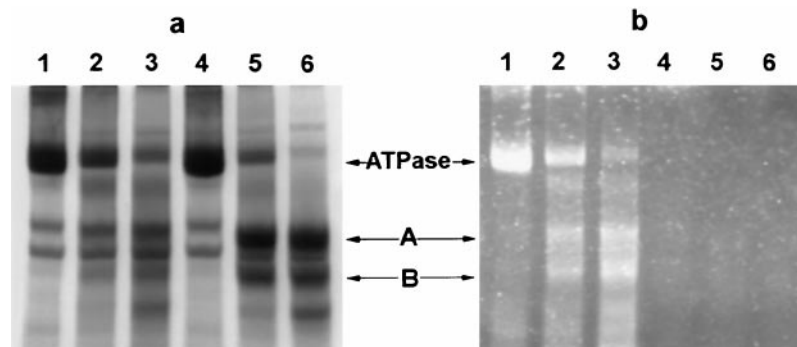
FIGURE 4   Distribution of reacted ThioGlo1 label in the cytosolic and membrane-bound regions of the ATPase. After incubation of SR vesicles with 100 μM ThioGlo1 for 30 min as described in the legend of Fig. 1, the reaction mixture was diluted to 0.04 mg SR protein/ml in 10 mM MOPS (pH 7.0) and 10% sucrose. The vesicles were sedimented in a refrigerated centrifuge at 100,000 $\times$ g for 45 min. The sediment was resuspended in 10 mM MOPS (pH 7.0), 10% sucrose to yield a concentration of ~2.0 mg protein/ml, in 50 mM Tris-Cl (pH 8.1), 0.25 M sucrose, and trypsin at a concentration (w/w) four times lower than that of the SR protein. This mixture was incubated for 10 min at 37°C, and the incubation was stopped with trypsin inhibitor (10-fold weight relative to trypsin). After centrifugation at 110,000 $\times$ g for 60 min, the supernatant containing the digested cytosolic region of the ATPase was collected, and the sediment was dissolved in 50 mM Tris-Cl (pH 8.1), 0.1% SDS. The fluorescence intensity of an undigested aliquot, as well as the supernatant and dissolved sediment of the digested sample, was then measured at an excitation wavelength of 379 nm. ▼, SR vesicles; ●, cytosolic region; ■, membrane-bound region.

SR protein in a medium containing 50 mM This/HCl (pH 8.1), 0.25 M sucrose, and 0.4 mg trypsin/ml. After a 15-min incubation at 37°C, the vesicles were centrifuged at 110,000 $\times$ g for 1 h, and the supernatant was further digested for 3 h at 37°C by adding 40 μg trypsin/ml. The resulting digests were subjected to high-performance liquid chromatography (HPLC) separation in a reverse-phase C18 column, using a linear gradient of 0.1% trifluoroacetic acid (TFA) in water and 0.1% TFA in 90% acetonitrile. Elution was monitored at 215 and 379 nm for peptide material and Tio-Glo label, respectively. The elution fractions exhibiting absorption at both 215 and 379 nm were collected and subjected to further HPLC purification, using a linear gradient of 10 mM NH4Ac (pH 6.5) and 10 mM NH4Ac in 90% acetonitrile. Elution was again monitored at 215 and 379 nm. The fractions were dried with Speedvac and subjected to mass spectrometric analysis.

Matrix-assisted laser desorption ionization (MALDI) analysis of tryptic peptides was performed on a Kratos (Manchester, UK) Kompakt MALDI III time-of-flight (TOF) mass spectrometer equipped with a nitrogen laser emitting at 337 nm. A 50 mM matrix solution was prepared by dissolving cyano-4-hydroxy-cinnamic acid (Aldrich, Milwaukee, WI) in 30:70 acetonitrile and 0.1% TFA in water. Speedvac-dried HPLC fractions were redissolved in the same type of solvent. Aliquots (0.3 μl) of both matrix and analyte solutions were mixed directly on the instrument probe, dried at atmospheric pressure and room temperature, and finally introduced into the mass spectrometer. Spectra were the averaged profiles of 100 laser shots obtained using linear mode and external calibration, which afforded a 0.2% accuracy or better.

RESULTS

Incubation of SR vesicles with ThioGlo1 results in time-dependent inactivation of the ATPase (Fig. 3 A). The level of inactivation is dependent on the stoichiometry of derivatization with ThioGlo1, extrapolating to approximately four residues per ATPase molecule (Fig. 3 B).

A useful property of ThioGlo1 is the development of intense fluorescence after reaction of its maleimide moiety with cysteine residues. Thereby, protein derivatization with ThyoGlo can be monitored by measurements of fluorescence. We then digested derivatized vesicles exhaustively with trypsin and separated the cytosolic ATPase region from the membrane-bound region by centrifugation. We found in these experiments that nearly all of the fluorescent label was recovered with the cytosolic region (Fig. 4).

Another way to demonstrate conveniently fluorescent labeling of the ATPase protein is SDS gel electrophoresis (Fig. 5). It is also possible to demonstrate by this method that fluorescent labeling involves both A and B fragments originating from mild trypsin digestion of the ATPase (Fig. 5).

Further characterization of the ATPase derivatized with ThioGlo1 was obtained by extensive digestion with trypsin, separation of the resulting peptides by HPLC, and identification of the fluorescent peptides by mass spectrometry. Analysis of four prominently fluorescent HPLC fractions (Table 1) indicated that Cys^{364}, Cys^{498}, and Cys^{636} were the

FIGURE 5   Electrophoretic display of labeled ATPase and tryptic fragments. After labeling with ThioGlo1 o (lanes 1, 2 and 3) as described in Fig. 2, or in the absence of labeling (*lanes 4–6*), SR vesicles were subjected to mild trypsin digestion (SR protein/trypsin ratio, 100) for 0 min (*lanes 1 and 4*), 1 min (*lanes 2 and 5*), or 6 min (*lanes 3 and 6*), at 25°C temperature. The digestion was stopped by the addition of trypsin inhibitor (inhibitor/trypsin ratio, 10). The digestion mixture contained 20 mM MOPS (pH 7.0), 80 mM KCl, 5 mM MgCl$_2$, and 0.7 mg SR protein/ml. Aliquots were then dissolved in 50 mM Tris (pH 8.1), 1% SDS and subjected to electrophoresis. (*a*) Protein stain. (*b*) Fluorescence emission.

TABLE 1 MALDI analysis of tryptic peptides by mass spectrometry

| HPLC fraction	Major spectral peak	Matched peptide	Calculated mass $[M + H]^+$
1	m/z 884	(M) $C_{498}SPAK_{502}$ + 379.3(ThioGlo1)	884
2	m/z 1342	(K) $G_{630}TAIAICRR_{638}$ + 379.3(ThioGlo1)	1340
4	m/z 818	(M) $S_{362}VCK_{365}$ + 379.3(ThioGlo1)	816
5	m/z 3745	(R) $[621 - 651]$ + 379.3(ThioGlo1)	3742

ThioGlo1-labeled ATPase was subjected to extensive trypsin digestion (see Materials and Methods), and the prominently fluorescent HPLC fractions were collected for mass spectrometry. Accuracy = 0.2%.

derivatized residues. Derivatization of these resides is consistent with fluorescent labeling of both large fragments A and B, which was observed in electrophoretic gels. The slightly higher level of labeling determined by fluorescence (i.e., approximately four residues) may be due to partial labeling of other residues or slightly inaccurate fluorometric determination of derivative stoichiometry.

ATPase inactivation by ThioGlo1 was not affected significantly by the presence or the absence of Ca^{2+}, whereas strong protection was observed upon addition of ATP (Fig. 6). A much lower protection was observed in the presence of p-nitrophenyl phosphate. Analogous results were obtained when ATPase derivatization with ThioGlo1 was assessed by fluorescence measurements. It is shown in Fig. 7 A that, in addition to ATP, TNP-AMP yields even stronger protection, whereas thapsigargin does not. Derivatization of
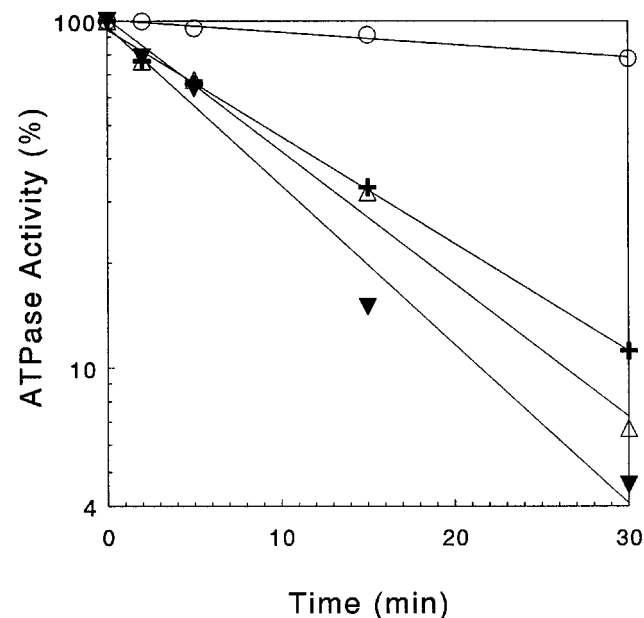
FIGURE 6 Time course of ATPase inactivation by ThioGlo1 in the presence of various ligands. Incubation with ThioGlo1 and sampling for ATPase determinations were carried out as explained in Fig. 2. ▼, control; △, 20 μM Ca^{2+} and no EGTA; ✚, 10 mM pNPP; ○, 4 mM ATP.
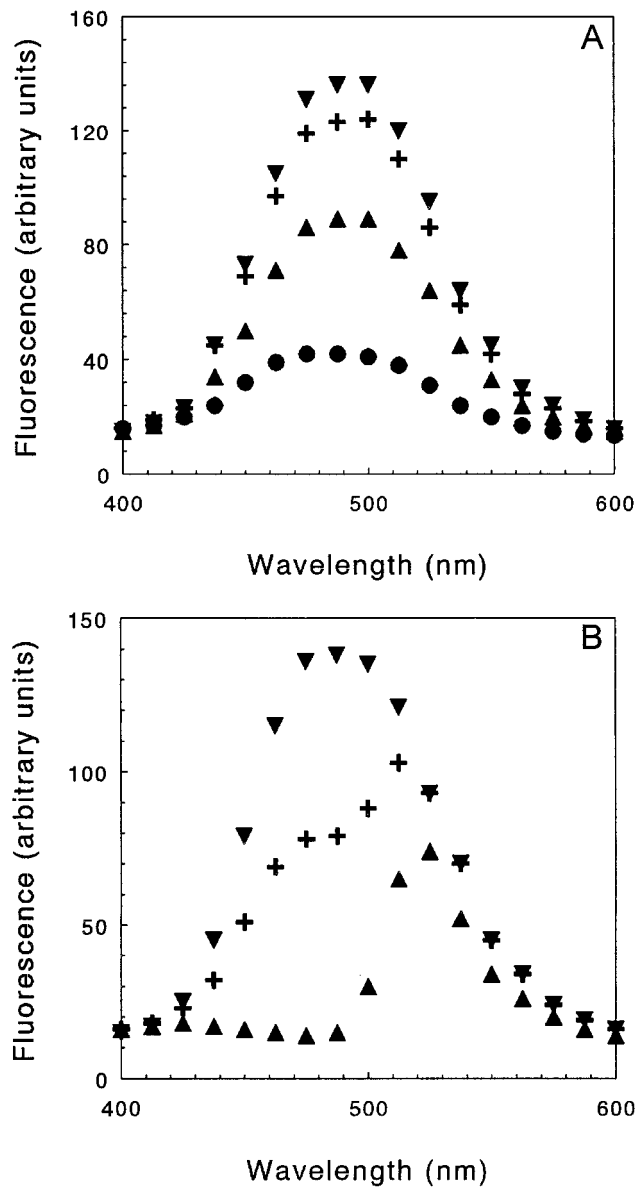
FIGURE 7 Fluorescent labeling of ATPase with Tho-Glo. (*A*) Effects of pNPP, ATP, and TNP-AMP. Incubation with 100 μM ThioGlo1 was carried out as explained in Fig. 2, with 20 mM MOPS (pH 7.0), 80 mM KCl, 5 mM $MgCl_2$, and 1 mM EGTA, in the absence (▼) or in the presence of 10 mM pNPP (✚), 4 mM ATP (▲), or 4 mM TNP-AMP (●). (*B*) Effect of prelabeling with FITC. Derivatization of Lys^{515} with FITC was obtained as described in Materials and Methods. The derivatized vesicles were sedimented by centrifugation and suspended in the ThioGlo1 reaction medium as described in *A*. Fluorescence of control vesicles was derivatized with ThioGlo1 (▼) only, FITC and then ThioGlo1 (✚), or FITC only (▲).

Lys^{515} with FITC (Pick and Karlish, 1980; Mitchinson et al., 1982) also has a protective effect (Fig. 7 *B*).

A most interesting finding is the strong protection by 0.6 mM vanadate, as opposed to the lack of protection by 100 mM phosphate (Fig. 8). It should be pointed out that such a concentration of phosphate, in the absence of Ca^{2+} (EGTA present) and K^+, and in the presence of 10 mM Mg^{2+}, is expected to allow reverse ATPase phosphorylation (Masuda
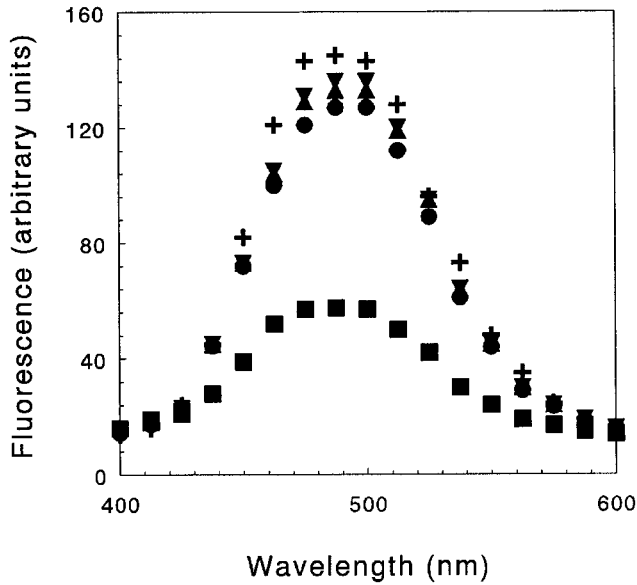
FIGURE 8 Fluorescent labeling of ATPase with ThioGlo1: effects of Ca²⁺, phosphate, TG, and vanadate. Incubation with 100 μM ThioGlo1 was carried out as explained in Fig. 2, in a reaction mixture containing 2 mM MOPS (pH 7), 80 mM KCl, 5 mM MgCl₂, and either 1 mM EGTA (▼) or 20 μM CaCl₂ (▲). Alternatively, the reaction mixture contained 20 mM MOPS (pH 7.0), 10 mM MgCl₂, 2 mM EGTA, and 100 mM phosphate (●), 50 μM TG (✚), or 0.6 mM vanadate (■). After 30 min of incubation, the samples were diluted to 50 μg protein/ml in 50 mM Tris (pH 8.1) and 0.1% SDS and placed in a fluorometer for determination of fluorescence intensity at an excitation wavelength of 379 nm.

and deMeis, 1973; Chaloub et al., 1979). Nearly identical patterns of derivatization were observed in the absence or in the presence of Ca²⁺ and thapsigargin (Fig. 8).

The influence of phosphate and vanadate on ATPase derivatization with ThioGlo1 was further characterized by gel electrophoresis. We found that both fluorescent labeling and the pattern of light digestion with trypsin were not affected significantly by phosphate (Fig. 9, c and d). On the other hand, the pattern of trypsin digestion of ATPase exposed to ThioGlo1 in the presence of vanadate was identical to that of control ATPase (compare Fig. 9, a and b).

Because SR ATPase is known to bind vanadate in the form of mono- or decavandate (Csermely et al., 1985; Varga et al., 1985), we performed further experiments using vanadate solutions made at pH 10 and pH 2 (Fig. 2) that are known to contain prevalently either monovanadate or decavanadate, respectively. In these experiments we obtained the same effects as those obtained with vanadate solutions made at neutral pH (Fig 10 A). When we used decavanadate at a concentration lower than the ATPase stoichiometry, we still obtained protection. This suggests that decavanadate (prepared at pH 2) undergoes significant breakdown when added to the neutral protein solution, and the resulting monovanadate affords protection. In fact, it was reported by Varga et al. (1985) that although decavanadate is stable at pH 2 and 2–4°C, breakdown to monovanadate occurs on the time scale of minutes if the pH and temperature are raised, as done in our experiments.

We then used various amounts of the monomer solution (prepared at pH 10) and found that the addition of monovanadate at a 1:1 stoichiometric ratio with the ATPase was sufficient to protect the enzyme from This-Glo (Fig. 10 B). This was evidently due to occupancy of the tight site reported by Csermely et al. (1985), who found that of two possible binding sites for monovanadate on the ATPase, only one manifests high affinity (apparent $K_d = 2$ μM), is not inhibited by derivatization of Lys⁵¹⁵ with FITC, and is not released by repeated washings. Assuming that the effects described above were due to monovanadate, we then

FIGURE 9 Electrophoretic display of labeled ATPase and tryptic fragments: protection by vanadate, but not by phosphate. Labeling with ThioGlo1 and collection of samples for electrophoresis were carried out as explained in Figs. 5 and 3, respectively. (a and c) Protein stain. (b and d) Fluorescence emission. Controls: 1, 2, and 3. Vanadate: 4, 5, and 6 in a and b. Phosphate: 4, 5, and 6 in c and d. Mild trypsin digestion: 0 for 1 and 4; 1 min for 2 and 5; 6 min for 3 and 6.
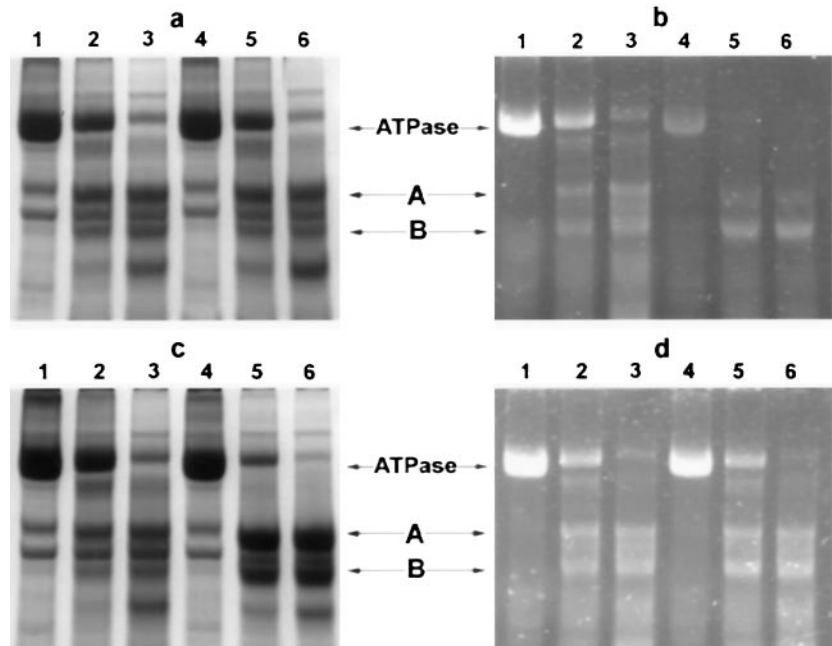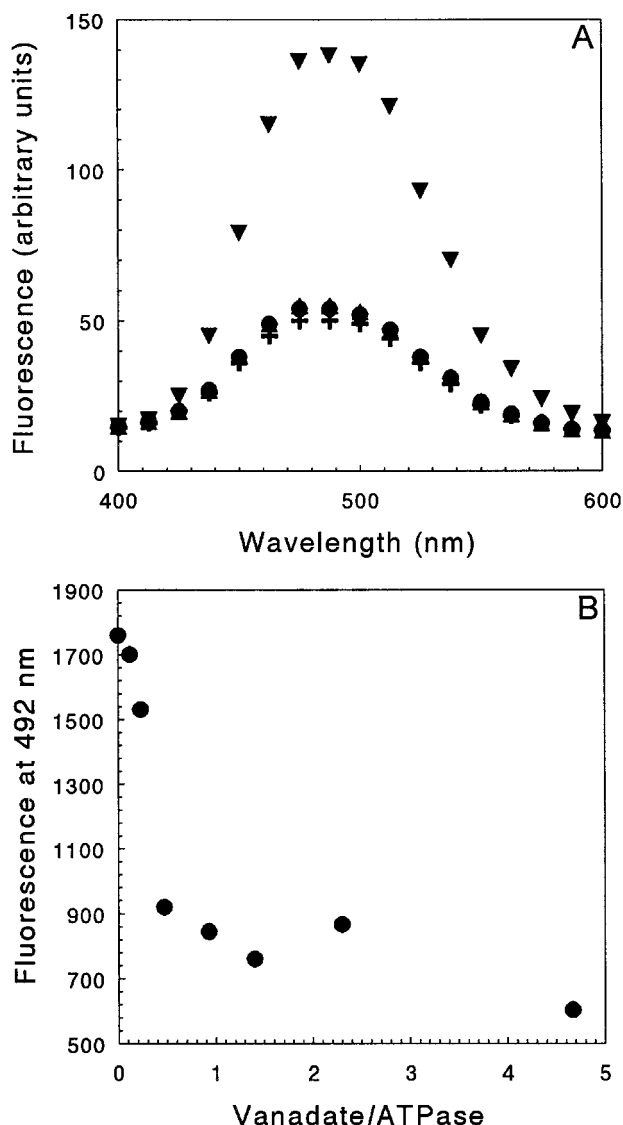
FIGURE 10 Fluorescent labeling of ATPase with ThioGlo1. (*A*) Comparative effects of monovanadate and decavanadate solutions. Derivatization of ATPase with 100 μM ThioGlo1 was carried out as explained in Fig. 2 in a reaction mixture containing 20 mM MOPS (pH 7.0), 10 mM MgCl$_2$, 2 mM EGTA in the absence (▼) or in the presence of 60 μM vanadate originally dissolved at pH 2 (✚) or pH 10 (●). (*B*) Enzyme inhibition as a function of the monovanadate:ATPase stoichiometric ratio.

checked whether protection from ThioGlo1 would be also observed under conditions favoring formation and conservation of decavanadate (Varga et al., 1985). To this end we made first a stock solution of decavanadate at pH 2.0 and then transferred an aliquot to a precooled (2–3°C) reaction mixture containing SR vesicles at neutral pH, to yield a decavanadate/ATPase stoichiometric ratio of 4. ThioGlo1 was then added for a 3.5-h incubation at 2–3°C, after which the protein was collected for determination of fluorescence. We found in these experiments that decavanadate had a protective effect that was very similar to that of monovanadate (not shown). We cannot exclude the possibility that

significant monovanadate concentrations may have been present even under these conditions.

DISCUSSION

Various maleimide-directed probes have been shown to label cysteine residues (Saito-Nakatsuka et al., 1987; Yamasaki et al., 1990; Bigelow and Inesi, 1991) within the cytosolic region of the ATPase, in close proximity to the phosphorylation and nucleotide-binding region. In our experiments, the dependence of inactivation on the stoichiometry of ThioGlo1 derivative extrapolated to approximately four residues per ATPase (Fig. 3). We observed (Fig. 5) fluorescent labeling of both fragments A and B obtained by light trypsin digestion of the ATPase (cut at Arg[505]) and identified Cys[364], Cys[498], and Cys[636] as the residues prominently labeled by ThioGlo1. Current models (Fig. 11) of the ATPase three-dimensional structure (Green, 1989; Green and Stokes, 1992; McIntosh, 1998; MacLennan et al., 1997; Yonekura et al., 1997) place these residues within the phosphorylation and nucleotide-binding region. In fact, protection is afforded by ATP or by Lys[515] derivatization with FITC, which is known to interfere with nucleotide binding (Mitchinson et al., 1982). Furthermore, strong protection is afforded by TNP-AMP, which is known to bind to the nucleotide site (Nakamoto and Inesi, 1984). On the other hand, protection of the ATPase by stoichiometric monovanadate is evidently related to formation of a pentacoordinated orthovandate complex at the phosphorylation site (Pick, 1982). This indicates that protection can also be obtained by occupancy of the phosphorylation site.

An intriguing question is whether protection by vanadate is directly related to its stabilization of the E2 conformation (Pick, 1982). Derivatization with ThioGlo1, however, occurs equally well in the presence and in the absence of Ca^{2+} (Fig. 8). This is consistent with the experiments of Seebregts and McIntosh (1989), who found that derivatization of Lys[492] with TNP-N3-nucleotide (also within the phosphorylation and nucleotide binding region) occurs equally well in the presence and in the absence of Ca^{2+}. Our findings are also consistent with the experiments of Green et al. (1977), who found that the reactivity of cysteine residues with DTNB was much reduced by the presence of substrate but hardly affected by Ca^{2+}.

The original definition of the E1 and E2 states is that the former is prevalent in the presence of Ca^{2+} and the second in the absence of Ca^{2+} (deMeis and Vianna, 1979). A profound functional difference between the so defined states is that E1 can be phosphorylated by ATP but not by inorganic phosphate, and E2 can be phosphorylated by inorganic phosphate but not by ATP. Spectroscopic evidence for a conformational difference between the so defined E1 and E2 states has been reported previously (see Bigelow and Inesi, 1992, and McIntosh, 1998, for reviews). However, our ThioGlo1 titrations proceed equally well in the presence or the absence of Ca^{2+}. We do not even see any protection
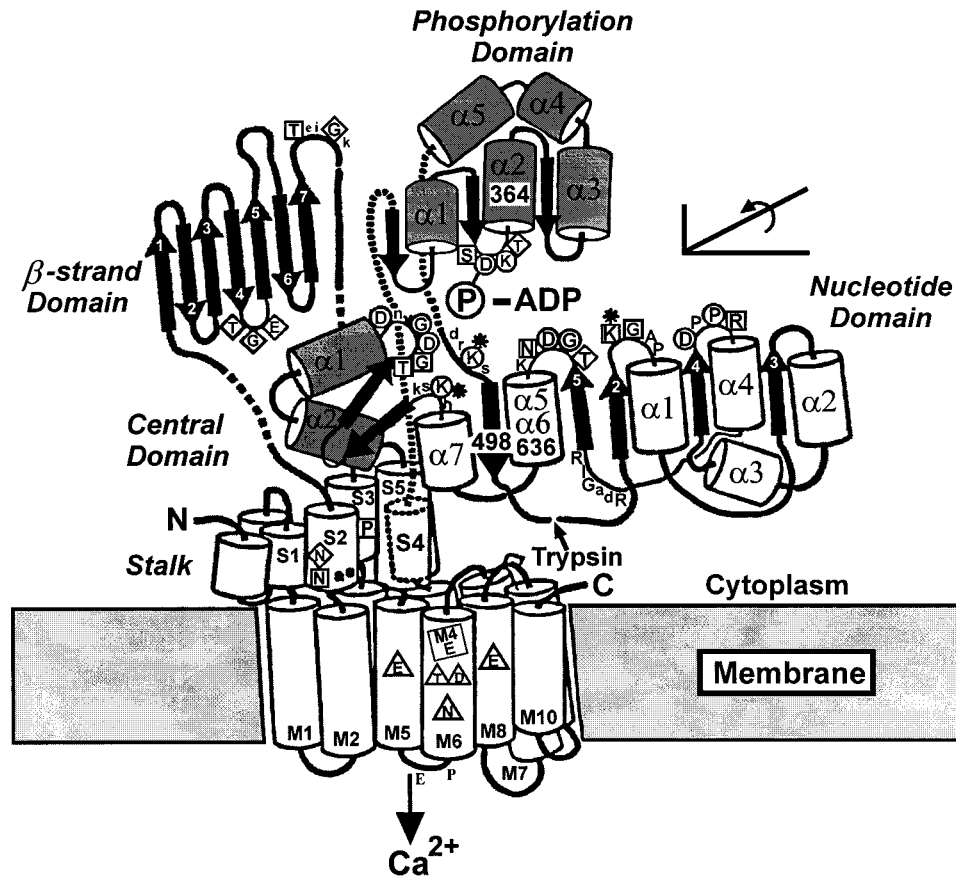
FIGURE 11 Topology of the ThioGlo1 reactive residues. The SR ATPase structural model is that proposed by Green and Stokes (1992), based on sequence alignment and consensus of secondary structure predictions (Green, 1989). The three ThioGlo1 reactive residues are all near the phosphorylation and nucleotide binding domain, within the large extramembranous region. The ThioGlo1 reactive C364 is placed distal to the Asp^{351} undergoing phosphorylation. The ThioGlo1 reactive C498 is proximal to the trypsin site (Arg^{505}) and distal to Lys^{492} (*asterisk*). Lys^{492} can be cross-linked with Lys^{515} (*asterisk*) by DIDS (Hua and Inesi, 1997), consistent with a 13 Å distance that is close to the length of the ATP molecule. Lys^{492} and Lys^{684} react with pyridoxal phosphate and nucleotide derivatives (Murphy, 1977; Yamamoto et al., 1988; Yamagata et al., 1993), consistent with their proximity to the phosphorylation site. Lys^{492} also reacts with TNP-8N3-AMP (McIntosh et al., 1992) and even more efficiently with TNP-2N3-AMP (Inesi et al., 1992a), explaining the highly protective effect of TNP-AMP from ThioGlo1. Lys^{515} is the residues that react with FITC (Mitchinson et al., 1982), whereby ATP binding is interfered with. The ThioGlo1 reactive Cys^{636} is placed on the $\alpha6$ C-terminal, distal to the trypsin site (Arg^{505}), thereby explaining the fluorescent labeling of both A and B trypsin fragments. The model folding is consistent with the cross-linking of Lys^{492} and Arg^{678} by gluteraldehyde (Ross and McIntosh, 1987a,b), indicating close proximity of these two residues. The membrane-bound region includes residues (*enclosed in triangles*) whose mutations interfere with Ca^{2+} binding (Clarke et al., 1989). Effects of mutations on other residues are denoted by circles (total inhibition), squares (reduced activity), and diamonds (no prominent effect).

by thapsigargin (Fig. 8), which is believed to provide strong and irreversible stabilization of the E2 state (Sagara et al., 1992; Witcome et al., 1995). Therefore, ATPase derivatization with ThioGlo1 is independent of whether the enzyme is in the E1 or the E2 state.

Assuming that the protective effect of vanadate is due to occupancy of the phosphorylation site, an important question is related to the lack of protection by phosphate under conditions favoring enzyme phosporylation:

What is the difference between the vanadate state and the state obtained by phosphorylation with Pi (E-P2)? From the functional point of view there are important differences: The equilibrium constant for enzyme phosphorylation with phosphate is close to 1 (i.e., half of the enzyme is not covalently phosphorylated, even in the presence of saturating phosphate), whereas the vanadate complex is stoicho-

metric. Furthermore, the enzyme phosphorylated with P_i can bind Ca^{2+} with high affinity (perhaps by reequilibration of the E1 and E2 states), whereby the phosphoenzyme is destablized and undergoes hydrolysis. On the contrary, vanadate reduces the affinity of the ATPase for Ca^{2+} (Inesi et al., 1984; Fernandez-Belda et al., 1986) as obtained by ATPase phosphorylation by ATP (E-P1), rather than by phosphate (E-P2), and its complex with the ATPase remains stable. Such functional features must have a structural counterpart, suggesting strong interaction of vanadate with the protein. It is possible that the vanadate trigonal bipyramidal structure corresponds to a stable stereo analog of a penta-coordinate transition state of the phosphorylation reaction, with intermediate features of the E-P1 and E-P2 states. The strong stability of its complex explains why vanadate affords better protection than phosphate.

We then consider two additional questions:

1. How does our ThioGlo1 titration relate to previous spectroscopic studies? Several studies (Dupont, 1976; Pick and Karlish, 1980; Guillain et al., 1982; Fernandez-Belda et al., 1984; Henderson et al., 1994) have shown the occurrence of Ca^{2+}-induced spectroscopic effects, providing good evidence for a Ca^{2+}-dependent conformational transition (i.e., E2 to E1) of the ATPase. On the other hand, other studies have provided evidence for phosphorylation-dependent conformational transitions. For instance, ATP utilization by SR vesicles in the presence of a subliminar detergent concentration is accompanied by reversible clearing of turbity, suggesting that the ATPase is better able to bind detergent when phosphorylated (Watanabe and Inesi, 1982). In the same study it was also demonstrated by fluorescence energy transfer measurements that the distance between neighboring ATPase molecules increases upon phosphorylation. Most importantly, microcalorimetric titrations (Schwarz and Inesi, 1997) indicate that large entropic effects are already associated with phosphate interaction with the ATPase in the E2 state. Consistent with these findings, our present titration with ThioGlo1 indicates that stable occupancy of the phosporylation site by vanadate affords strong protection of the phosphorylation and nucleotide-binding region. It is then apparent that two conformational transitions may occur, one due to Ca^{2+} binding and the other to phosphorylation. From the functional standpoint, the former would be involved in enzyme activation, and the latter would trigger a change in Ca^{2+}-binding affinity and vectorial exposure. Although the field of cation transport ATPases has been dominated by an interest in the Ca^{2+}-induced (E2-to-E1) transition, the fact is that an E-to-E-P transition must also occur to account for energy transduction.

2. How do our ThioGlo titrations relate to recent diffraction studies? A useful aspect of our titrations is that they provide evidence of vanadate effects on ATPase, independent of crystallization requirements. These effects can then be used in attempts to establish a correspondence between structural images derived from diffraction studies and functionally defined enzyme states. There is no doubt that both the ThioGlo1 titration pattern (this study) and the diffraction image (Ogawa et al., 1998) obtained in the presence of Ca^{2+} and in the absence of vanadate correspond to the E1 state. On the other hand, the structural image obtained from ATPase tubular crystal formed in the absence of Ca^{2+} must be considered in the light of the requirement for vanadate (or rather decavanadate) to obtain such crystals (Dux and Martonosi, 1983; Zhang et al., 1998). Monovanadate and decavanadate appear to be similarly protective with regard to ATPase derivatization with ThioGlo1, although the presence of low concentrations of monovanadate in the decavanadate experiments cannot be excluded. The high ionization charge of decavanadate has the additional effect of stabilizing ATPase arrays that are suitable for electron diffraction. Diffraction studies and titrations with ThioGlo1 both demonstrate that highly significant changes are produced by vanadate within the cytosolic region of the ATPase. The criteria discussed above raise the possibility that specific structural features observed in the presence of vanadate may not be due to the fact that the enzyme resides in the E2 state, but rather correspond to a stable transition-state analog of the phosphorylation reaction. It is likely that this state, as characterized by the distinct structural image obtained by diffraction studies (Ogawa et al., 1998), is of functional relevance in the progress of the catalytic and transport cycle following phosphorylation of the Ca^{2+}-activated enzyme by ATP.

REFERENCES

Bigelow, D. J., and G. Inesi. 1991. Frequency-domain fluorescence spectroscopy resolves the location of maleimide-directed spectroscopic probes within the tertiary structure of the Ca-ATPase of sarcoplasmic reticulum. *Biochemistry.* 30:2113–2125.

Bigelow, D. J., and G. Inesi. 1992. Contributions of chemical derivatization and spectroscopic studies to the characterization of the Ca^{2+} transport ATPase of sarcoplasmic reticulum. *Biochim. Biophys. Acta Biomembr.* 1113:323–338.

Chaloub, R. M., H. Guimaraes-Motta, S. Verjovski-Almeida, L. deMeis, and G. Inesi. 1979. Sequential reactions in P_i utilization for ATP synthesis by sarcoplasmic reticulum. *J. Biol. Chem.* 254:9464–9468.

Clarke, D. M., T. W. Loo, G. Inesi, and D. H. MacLennan. 1989. Location of high affinity Ca^{2+}-binding sites within the predicted transmembrane domain of the sarcoplasmic reticulum Ca^{2+}-ATPase. *Nature.* 339:476–478.

Csermely, P., S. Varga, and A. Martonosi. 1985. Competition between decavanadate and fluorescein isothiocyanate in the Ca^{2+}-ATPase of sarcoplasmic reticulum. *Eur. J. Biochem.* 150:455–460.

deMeis, L., and A. Vianna. 1979. Energy interconversion by the Ca^{2+}-dependent ATPase of the sarcoplasmic reticulum. *Annu. Rev. Biochem.* 48:275–292.

Dupont, Y. 1976. Fluorescence studies of the sarcoplasmic reticulum calcium pump. *Biochem. Biophys. Res. Commun.* 71:544–550.

Dux, L., and A. Martonosi. 1983. Two dimensional arrays of proteins in sarcoplasmic reticulum and purified Ca^{2+}-ATPase vesicles treated with vanadate. *J. Biol. Chem.* 258:2599–2603.

Eletr, S., and G. Inesi. 1972. Phospholipid orientation in sarcoplasmic reticulum membranes: spin label and proton NMR studies. *Biochim. Biophys. Acta.* 282:174–179.

Fernandez-Belda, F. J., J. Garcia de Ancos, and G. Inesi. 1986. Fluorometric titration of the sarcoplasmic reticulum adenosine triphosphatase calcium sites in the presence of vanadate. *Biochim. Biophys. Acta.* 854:257–264.

Fernandez-Belda, F. J., M. Kurzmack, and G. Inesi. 1984. A comparative study of calcium transients by isotopic tracer, metallochromic indicator, and intrinsic fluorescence in sarcoplasmic reticulum ATPase. *J. Biol. Chem.* 259:9687–9698.

Green, N. M. 1989. ATP-driven cation pumps: alignment of sequences. *Biochem. Soc. Trans.* 17:972–972.

Green, N. M., G. Allen, G. M. Hebdon, and D. A. Thorley-Lawson. 1977. Structural studies on the Ca^{2+} transporting ATPase of sarcoplasmic reticulum. *In* Ca^{2+} Binding Proteins and Ca^{2+} Function. R. H. Wasserman et al., editors. Elsevier North-Holland, Amsterdam. 164–172.

Green, N. M., and D. L. Stokes. 1992. Structural modelling of P-type ion pumps. *Acta Physiol. Scand.* 146(Suppl. 607):59–68.

Guillain, F., M. P. Gingold, and P. Champeil. 1982. Direct fluorescence measurements of Mg^{2+} binding to sarcoplasmic reticulum ATPase. *J. Biol. Chem.* 257:7366–7371.

Henderson, I. M. J., Y. M. Khan, J. M. East, and A. G. Lee. 1994. Binding of Ca^{2+} to the $(Ca^{2+}-Mg^{2+})$-ATPase of sarcoplasmic reticulum: equilibrium studies. *Biochem. J.* 297:615–624.

Hua, S., and G. Inesi. 1997. Synthesis of a radioactive azido derivative of thapsigargin and photolabeling of the sarcoplasmic reticulum ATPase. *Biochemistry.* 36:11865–11872.

Inesi, G., T. Cantilina, X. Yu, D. Nikic, Y. Sagara, and M. E. Kirtley. 1992a. Long range intramolecular linked functions in activation and inhibition of SERCA ATPases. *Ann. N.Y. Acad. Sci.* 671:32–49.

Inesi, G., D. Lewis, and A. J. Murphy. 1984. Interdependence of H^+, Ca^{2+} and P_i (or vanadate) sites in sarcoplasmic reticulum ATPase. *J. Biol. Chem.* 259:996–1003.

Inesi, G., D. Lewis, D. Nikic, and M. E. Kirtley. 1992b. Long range intramolecular linked functions in the calcium transport ATPase. *In* Advances in Enzymology. A. Meister, editor. John Wiley and Sons, New York. 185–215.

Lanzetta, P. A., L. J. Alvarez, P. S. Reinsch, and O. A. Candia. 1979. An improved assay for nanomole amounts of inorganic phosphate. *Anal. Biochem.* 100:95–97.

Lowry, O. H., N. J. Roseborough, A. L. Farr, and R. J. Randall. 1951. Protein measurement with the Folin phenol reagent. *J. Biol. Chem.* 193:265–275.

MacLennan, D. H., W. J. Rice, and N. M. Green. 1997. The mechanism of Ca^{2+} transport by sarco(endo)plasmic reticulum Ca^{2+} ATPases. *J. Biol. Chem.* 272:28815–28818.

Masuda, H., and L. deMeis. 1973. Phosphorylation of the sarcoplasmic reticulum membrane by orthophosphate. Inhibition by calcium ions. *Biochemistry.* 12:4581–4585.

McIntosh, D. B. 1998. The ATP Binding Sites of P-Type Ion Transport ATPases: Properties, Structure, Conformations, and Mechanism of Energy Coupling. *In* Advances in Molecular and Cell Biology. JAI Press, Greenwich, CT. 33–99.

McIntosh, D. B., D. G. Woolley, and M. C. Berman. 1992. $2',3'-O$-(2,4,6-trinitrophenyl)-8-azido-AMP and -ATP photolabel Lys-492 at the active site of sarcoplasmic reticulum Ca^{2+}-ATPase. *J. Biol. Chem.* 267:5301–5309.

Mitchinson, C., A. Wilderspin, B. J. Trinnaman, and N. M. Green. 1982. Identification of a labelled peptide after stoicheiometric reaction of fluorescein isothiocyanate with the Ca^{2+} dependent adenosine triphosphatase of sarcoplasmic reticulum. *FEBS Lett.* 146:87–92.

Murphy, A. J. 1976. Sulfhydryl group modification of sarcoplasmic reticulum. *Biochemistry.* 15:4492–4496.

Murphy, A. J. 1977. Sarcoplasmic reticulum adenosine triphosphatase: labeling of an essential lysyl residue with pyroxidal-$5'$-phosphate. *Arch. Biochem. Biophys.* 180:114–120.

Murphy, A. J. 1978. Effects of divalent cations and nucleotides on the reactivity of the sulfhydryl groups of sarcoplasmic reticulum membranes. *J. Biol. Chem.* 253:385–389.

Nakamoto, R. K., and G. Inesi. 1984. Studies of the Interactions of $2',3'-O$-(2,4,6-trinitrocyclohexyldienylidine)adenosine nucleotides with the sarcoplasmic reticulum $(Ca^{2+} + Mg^{2+})$-ATPase active site. *J. Biol. Chem.* 259:2961–2970.

Ogawa, H., D. L. Stokes, H. Sasabe, and C. Toyoshima. 1998. Structure of the Ca^{2+} pump of sarcoplasmic reticulum: a view along the lipid bilayer at 9-Å resolution. *Biophys. J.* 75:41–52.

Pick, U. 1982. The interaction of vanadate ions with the Ca-ATPase from sarcoplasmic reticulum. *J. Biol. Chem.* 257:6111–6119.

Pick, U., and S. J. Karlish. 1980. Indications for an oligomeric structure and for conformational changes in sarcoplasmic reticulum Ca^{2+}-ATPase labelled selectively with fluorescein. *Biochim. Biophys. Acta.* 626:255–261.

Ross, D. C., and D. B. McIntosh. 1987a. Intramolecular cross-linking of domains at the active site links A1 and B subfragments of the Ca^{2+}-ATPase of sarcoplasmic reticulum. *J. Biol. Chem.* 262:2042–2049.

Ross, D. C., and D. B. McIntosh. 1987b. Intramolecular cross-linking at the active site of the Ca^{2+}-ATPase of sarcoplasmic reticulum. *J. Biol. Chem.* 262:12977–12983.

Sagara, Y., J. B. Wade, and G. Inesi. 1992. A conformational mechanism for formation of a dead-end complex by the sarcoplasmic reticulum ATPase with thapsigargin. *J. Biol. Chem.* 267:1286–1292.

Saito-Nakatsuka, K., T. Yamashita, I. Kubota, and M. Kawakita. 1987. Reactive sulfhydryl groups of sarcoplasmic reticulum ATPase. I. Location of a group which is most reactive with *N*-ethylmaleimide. *J. Biochem. (Tokyo).* 101:365–376.

Schwarz, F. P., and G. Inesi. 1997. Entropic drive in the sarcoplasmic reticulum ATPase interacion with Mg^{2+} and P_i. *Biophys. J.* 73:2179–2182.

Seebregts, C. J., and D. B. McIntosh. 1989. $2',3'-O$-(2,4,6-trinitrophenyl)-8-azido-adenosine mono-, di-, and triphosphates as photoaffinity probes of the Ca^{2+}-ATPase of sarcoplasmic reticulum. Regulatory/superfluorescent nucleotides label the catalytic site with high efficiency. *J. Biol. Chem.* 264:2043–2052.

Squier, T. C., D. J. Bigelow, J. Garcia de Ancos, and G. Inesi. 1987. Localization of site-specific probes on the Ca-ATPase of sarcoplasmic reticulum vesicles using fluorescence energy transfer. *J. Biol. Chem.* 262:4748–4754.

Varga, S., P. Csermely, and A. Martonosi. 1985. The binding of vanadium (V) oligoanions to sarcoplasmic reticulum. *Eur. J. Biochem.* 148:119–126.

Watanabe, T., and G. Inesi. 1982. Structural effects of substrate utilization on the ATPase chains of sarcoplasmic reticulum. *Biochemistry.* 21:3254–3259.

Weber, K., and M. Osborn. 1969. The reliability of molecular weight determinations by dodecyl sulfate-polyacrylamide gel electrophoresis. *J. Biol. Chem.* 244:4406–4417.

Witcome, M., Y. M. Khan, M. East, and A. G. Lee. 1995. Binding of sesquiterpene lactone inhibitors to the Ca^{2+}-ATPase. *Biochem. J.* 310:859–868.

Yamagata, K., T. Daiho, and T. Kanazawa. 1993. Labeling of lysine 492 with pyridoxal $5'$-phosphate in the sarcoplasmic reticulum Ca^{2+}-ATPase. Lysine 492 residue is located outside the fluorescein 5-isothiocyanate-binding region in or near the ATP binding site. *J. Biol. Chem.* 268:20930–20936.

Yamamoto, H., M. Tagaya, T. Fukui, and M. Kawakita. 1988. Affinity labelling of the ATP-binding site of Ca^{2+}-transporting ATPase of sarcoplasmic reticulum by adenosine triphosphopyridoxal: identification of the reactive lysyl residue. *J. Biochem. (Tokyo).* 103:452–457.

Yamasaki, K., N. Sano, M. Ohe, and T. Yamamoto. 1990. Determination of the primary structure of intermolecular cross-linking sites on the Ca^{2+}-ATPase of sarcoplasmic reticulum using ^{14}C-labeled N,N'-(1,4-phenylene)bismaleimide or *N*-ethylmaleimide. *J. Biochem. (Tokyo).* 108:918–925.

Yonekura, K., D. L. Stokes, H. Sasabe, and C. Toyoshima. 1997. The ATP-binding site of Ca(2+)-ATPase revealed by electron image analysis. *Biophys. J.* 72:997–1005.

Zhang, P., C. Toyoshima, K. Yonekura, N. M. Green, and D. L. Stokes. 1998. Structure of the calcium pump from sarcoplasmic reticulum at 8-Å resolution. *Nature.* 392:835–839.